

Cobalt(II), copper(II), zinc(II) and palladium(II) Schiff base complexes: Synthesis, characterization and catalytic performance in selective oxidation of sulfides using hydrogen peroxide under solvent-free conditions



Mahsa Khorshidifard^a, Hadi Amiri Rudbari^{a,*}, Banafshe Askari^a, Mehdi Sahihi^a, Mostafa Riahi Farsani^b, Fariba Jalilian^a, Giuseppe Bruno^c

^a Department of Chemistry, University of Isfahan, Isfahan 81746-73441, Iran

^b Young Researchers and Elite Club, Islamic Azad University, Shahrekord Branch, Shahrekord, Iran

^c Department of Chemical Sciences, University of Messina, Via F. Stagno d'Alcontres 31, 98166 Messina, Italy

ARTICLE INFO

Article history:

Received 25 January 2015

Accepted 28 March 2015

Available online 14 April 2015

Keywords:

Schiff base

Crystal structure

Oxidation of sulfide

H₂O₂

Solvent free

ABSTRACT

An asymmetric bidentate Schiff-base ligand (**HL**: 2-*tert*-butyliminomethyl-phenol) was prepared from the reaction of salicylaldehyde and *tert*-butylamine. Cobalt(II), copper(II), zinc(II) and Pd(II) complexes, **CoL₂**, **CuL₂**, **ZnL₂** and **PdL₂**, were synthesized from the reaction of CoCl₂·6H₂O, CuCl₂·2H₂O, Zn(NO₃)₂·6H₂O and PdCl₂ with the bidentate Schiff base ligand **HL** in methanol. The ligand and its metal complexes were characterized by elemental analysis (CHN), FT-IR and UV-Vis spectroscopy. In addition, ¹H and ¹³C NMR techniques were employed for characterization of the ligand (**HL**) and the diamagnetic complexes (**ZnL₂** and **PdL₂**). The molecular structures of all the complexes were determined by the single crystal X-ray diffraction technique. The crystallographic data reveal that in all the complexes the metal centers are four-coordinated by two phenolate oxygen and two imine nitrogen atoms of two Schiff base ligands. The geometry around the metal center in the **CoL₂**, **CuL₂** and **ZnL₂** complexes is a distorted tetrahedral and for **PdL₂** it is square-planar.

The catalytic activity of these complexes has been evaluated for the selective oxidation of sulfides with the green oxidant 35% aqueous H₂O₂ under solvent free conditions. For all the catalysts, using optimized reaction conditions, different sulfides were converted to the corresponding sulfones. **ZnL₂** showed a higher catalytic performance for the oxidation of the different sulfides to the corresponding sulfones.

© 2015 Elsevier Ltd. All rights reserved.

1. Introduction

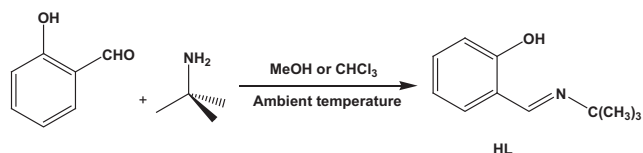
The selective oxidation of organosulfur compounds has attracted much attention from the viewpoint of organizing chemical processes for the preparation of synthetically useful sulfoxides, and sulfones, which are important and versatile intermediates in the synthesis of natural products and biologically significant molecules [1,2], ligands in asymmetric catalysis [3] and oxo-transfer reagents [4,5]. Among a lot of different oxidants, aqueous hydrogen peroxide has been one of the most noteworthy “green oxidants”, offering the advantages of safety in storage and operation, being cheap, readily available, of highly effective oxygen content and environmentally benign, with the formation of water as the only

by-product [6]. Different catalysts, such as polyoxometallates and transition-metal Schiff-base complexes, have been used for H₂O₂-based oxidation of sulfides [7–20]. However, the oxidation of sulfides to sulfones has been much less investigated as compared to the oxidation of sulfides to sulfoxides. Also, many of these systems suffer from one or more limitations, such as high cost, the requirement of a promoter or a co-catalyst, high temperature, long reaction time, chlorohydrocarbon solvents and excessive H₂O₂. These defects are becoming more apparent in view of the developing environmental concerns in recent years [7,10,11]. In addition, most of the catalysts are required to use a solvent in the reaction, while it is highly favorable to expand a process without a solvent from the viewpoint of green chemistry.

Schiff base ligands have played an important role in the development of coordination chemistry, especially their metal complexes exhibit wide applications in biological and industrial

* Corresponding author. Tel.: +98 31 37934918.

E-mail addresses: h.a.rudbari@sci.ui.ac.ir, hamiri1358@gmail.com (H.A. Rudbari).



Scheme 1. Synthesis of the ligand (HL).

systems [21–26]. Furthermore, Schiff bases are very important tools for inorganic chemists, as they are widely used to design molecular ferromagnets, in catalysis, in biological modeling applications, as liquid crystals and as heterogeneous catalysts [27–29]. Unfortunately, application of Schiff base complexes as a catalyst for the solvent-free oxidation of sulfides with hydrogen peroxide is very rare [30–33].

So current demand for environmentally friendly processes requires the synthesis of new catalysts and the development of green oxidation methods that use clean oxidants, such as hydrogen peroxide, without any solvent. As part of our research program on the synthesis, characterization and catalytic activity of Schiff base ligands and complexes [34–37], in this paper, we synthesized a bidentate Schiff base ligand, **HL**, derived from salicylaldehyde and *tert*-butylamine (Scheme 1). In order to investigate the coordination modes of this ligand, cobalt(II), copper(II), zinc(II) and palladium(II) complexes were synthesized (Scheme 2). After synthesis and characterization of the complexes, we used them in the no-solvent oxidation of sulfides with hydrogen peroxide as a green oxidant. This process is clean, safe, selective, simple and cost-effective for the oxidation of sulfides to the corresponding sulfones.

2. Experimental section

2.1. Chemicals and instrumentation

All the chemicals were purchased from Merck Co. and used without further purification. The FT-IR spectra were recorded on a JASCO, FT/IR-6300 spectrometer ($4000\text{--}400\text{ cm}^{-1}$) in KBr pellets. ^1H and ^{13}C NMR spectra were recorded on a Bruker Avance 400 spectrometer using CDCl_3 (for the palladium(II) complex) and $\text{DMSO-}d_6$ (for the ligand and zinc(II) complex) as solvents. The elemental analysis was performed on Leco, CHNS-932 and Perkin-Elmer 7300 DV elemental analyzers. UV–Vis spectra were recorded on a JASCO V-670 UV–Vis spectrophotometer ($200\text{--}700\text{ nm}$). The oxidation products were quantitatively analyzed by gas chromatography (GC) on a Shimadzu GC-16A instrument using a 2 m column packed with silicon DC-200 and an FID detector.

2.2. Single crystal diffraction studies

X-ray data for complexes, **CoL₂**, **CuL₂**, **ZnL₂** and **PdL₂**, were collected on a STOE IPDS-II diffractometer with graphite monochromated Mo $K\alpha$ radiation. For **CuL₂**, **CoL₂**, **ZnL₂** and **PdL₂** the

crystals were dark green, red, yellow and light red, respectively. A high-quality piece of crystal was chosen in each case using a polarizing microscope and they were mounted on a glass fiber, then used for data collection. Cell constants and an orientation matrix for data collection were obtained from the least-squares refinement of diffraction data from 5922 for **CuL₂**, 3108 for **CoL₂**, 3501 for **ZnL₂** and 2450 for **PdL₂** unique reflections. Data were collected at a temperature of 298(2) K in a series of ω scans in 1° oscillations and integrated using the Stöe X-Area software package [38]. A numerical absorption correction was applied using the X-RED [39] and X-SHAPE [39] software packages. The data were corrected for Lorentz and Polarizing effects. The structures were solved by direct methods using SIR2004 [40]. The non-hydrogen atoms were refined anisotropically by the full matrix least squares method on F^2 using SHELXL [41]. All hydrogen atoms were added at ideal positions and constrained to ride on their parent atoms.

In the crystal structures of **CoL₂** and **ZnL₂**, the C9, C10 and C11 carbon atoms of the *tert*-butyl group were disordered over two sites and refined with site occupancy factors 0.67:0.33 and 0.65:0.35 for **CoL₂** and **ZnL₂**, respectively (details are available in the archived CIF). Crystallographic data for the complexes are listed in Table 1. Selected bond distances and angles are summarized in Table 2.

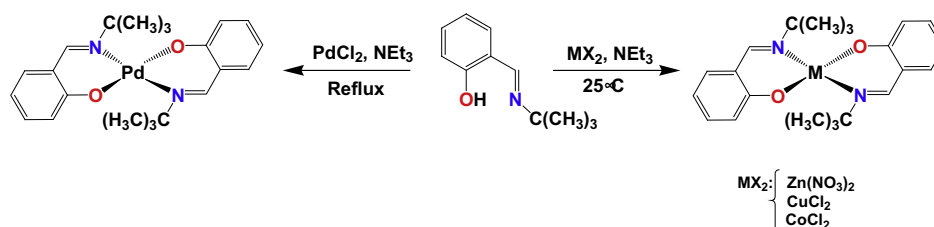
2.3. Synthesis of the Schiff-base ligand (**HL**: 2-*tert*-butyliminomethylphenol)

Tert-butylamine (10 mmol) was dissolved in 30 ml of absolute methanol or chloroform and was added slowly to a stirring solution of salicylaldehyde (10 mmol) in 30 ml of absolute methanol or chloroform at ambient temperature. The color immediately changed to yellow. The mixture was then stirred for 2 h at ambient temperature before removal of the solvent under vacuum. The result was a yellow oil. Yield 89%, *Anal. Calc.* for $\text{C}_{11}\text{H}_{15}\text{ON}$: C, 74.54; H, 8.53; N, 7.90. Found: C, 74.49; H, 8.56; N, 7.88%. FT-IR (KBr, cm^{-1}): 3480 ($\nu_{\text{O-H}}$, br, vs), 3060–2871 (C–H aliphatic and aromatic), 1628 ($\nu_{\text{C=N}}$), 1196 ($\nu_{\text{C-O}}$). ^1H and ^{13}C NMR ($\text{DMSO-}d_6$, 400 MHz, 298 K): Table 3.

2.4. Preparation of the complexes

General procedures for the preparation of **CoL₂**, **CuL₂**, **ZnL₂** and **PdL₂**.

A MeOH solution (20 cm^3) of *tert*-butylamine (2 mmol) was added dropwise to a MeOH solution (20 cm^3) of the salicylaldehyde (2 mmol). The yellow solution was stirred for 2 h at ambient temperature, then a solution of triethylamine (3 mmol) in absolute MeOH (5 cm^3) was added to the solution. The solution turned dark yellow and was stirred for 10 min, then a solution of the appropriate metal salt (1 mmol) in absolute MeOH (20 cm^3) was added dropwise. The resulting solution was stirred for 12 h at ambient temperature for the preparation of the **CoL₂**, **CuL₂** and **ZnL₂** complexes, while for the palladium(II) complex, **PdL₂**, the solution was refluxed overnight.



Scheme 2. Synthetic routes for the preparation of the complexes.

Table 1
Crystal data and structure refinement.

	CuL₂	CoL₂	PdL₂	ZnL₂
Empirical formula	C ₂₂ H ₂₈ N ₂ O ₂ Cu	C ₂₂ H ₂₈ N ₂ O ₂ Co	C ₂₂ H ₂₈ N ₂ O ₂ Pd	C ₂₂ H ₂₈ N ₂ O ₂ Zn
Formula weight	416.00	411.39	458.86	417.83
<i>T</i> (K)	298(2)	298(2)	298(2)	298(2)
λ (Å)	0.71073	0.71073	0.71073	0.71073
Crystal system	orthorhombic	orthorhombic	monoclinic	monoclinic
Space group	<i>P</i> 2(1)2(1)2(1)	<i>P</i> ca2(1)	<i>C</i> 2/ <i>c</i>	<i>P</i> 2(1)
Unit cell dimensions				
<i>a</i> (Å)	9.1377(18)	20.1258(14)	19.308(2)	10.625(2)
<i>b</i> (Å)	11.192(2)	10.9506(8)	7.7468(7)	9.982(2)
<i>c</i> (Å)	21.367(4)	9.8769(9)	14.6967(16)	10.821(2)
β (°)			108.753(9)	110.81(3)
<i>V</i> (Å ³)	2185.3(8)	2176.8(3)	2081.6(4)	1072.8(4)
<i>Z</i>	4	4	4	2
<i>D</i> _{calc} (Mg m ^{−3})	1.264	1.255	1.464	1.294
Absorption coefficient (mm ^{−1})	1.017	0.806	0.910	1.162
<i>F</i> (000)	876	868	944	440
θ range for data, collection	2.42–25.00	2.75–29.38	2.86–28.00	2.87–25.00
Index ranges	−12 ≤ <i>h</i> ≤ 12 −15 ≤ <i>k</i> ≤ 15 0 ≤ <i>l</i> ≤ 29	0 ≤ <i>h</i> ≤ 27 −15 ≤ <i>k</i> ≤ 0 0 ≤ <i>l</i> ≤ 13	−25 ≤ <i>h</i> ≤ 24 0 ≤ <i>k</i> ≤ 10 0 ≤ <i>l</i> ≤ 19	−12 ≤ <i>h</i> ≤ 12 −10 ≤ <i>k</i> ≤ 11 −12 ≤ <i>l</i> ≤ 12
Reflections collected	11 776	3108	2450	9535
Independent reflections	5922 [<i>R</i> _{int}] = 0.0277]	3108 [<i>R</i> _{int}] = 0.0473]	2450 [<i>R</i> _{int}] = 0.0217]	3501 [<i>R</i> _{int}] = 0.0456]
Data completeness (%)	99.6	98.1	97.5	99.9
Refinement method	Full-matrix least-squares on <i>F</i> ²	Full-matrix least-squares on <i>F</i> ²	Full-matrix least-squares on <i>F</i> ²	Full-matrix least-squares on <i>F</i> ²
Data/restraints/parameters	5922/0/244	3108/1/275	2450/0/128	3501/1/272
Goodness-of-fit (GOF) on <i>F</i> ²	0.945	0.906	0.993	0.954
Final <i>R</i> indices [<i>I</i> > 2σ(<i>I</i>)]	<i>R</i> ₁ = 0.0319 <i>wR</i> ₂ = 0.0664	<i>R</i> ₁ = 0.0278 <i>wR</i> ₂ = 0.0687	<i>R</i> ₁ = 0.0379 <i>wR</i> ₂ = 0.1204	<i>R</i> ₁ = 0.0268 <i>wR</i> ₂ = 0.0382
<i>R</i> indices (all data)	<i>R</i> ₁ = 0.0522 <i>wR</i> ₂ = 0.0695	<i>R</i> ₁ = 0.589 <i>wR</i> ₂ = 0.0718	<i>R</i> ₁ = 0.0550 <i>wR</i> ₂ = 0.1243	<i>R</i> ₁ = 0.0447 <i>wR</i> ₂ = 0.0404
Largest difference in peak and hole (e Å ^{−3})	0.172 and −0.463	0.169 and −0.316	0.798 and −0.800	0.118 and −0.156

Table 2
Selected bond distances (Å) and angles (°) for **CuL₂**, **CoL₂**, **ZnL₂** and **PdL₂**.

	CuL ₂	CoL ₂	ZnL ₂		PdL ₂
M(1)–O(1)	1.8957(17)	1.883(3)	1.911(2)	Pd(1)–O(1)	1.987(3)
M(1)–N(1)	1.995(2)	2.003(3)	2.0200(19)	Pd(1)–N(1)	2.066(3)
N(1)–C(7)	1.285(3)	1.272(4)	1.275(4)	N(1)–C(7)	1.285(5)
N(2)–C(18)	1.286(3)	1.281(4)	1.272(3)		
O(1)–M(1)–O(2)	137.28(9)	113.66(12)	114.19(9)	O(1)–Pd(1)–O(1A)	180.00(17)
O(1)–M(1)–N(1)	95.88(8)	97.94(12)	97.58(11)	O(1)–Pd(1)–N(1)	88.45(12)
O(2)–M(1)–N(1)	100.18(7)	113.45(11)	96.65(9)	O(1)–Pd(1)–N(1A)	91.55(12)
N(1)–M(1)–N(2)	145.58(8)	122.03(12)	126.95(13)	N(1)–Pd(1)–N(1A)	180.0
O(2)–M(1)–N(2)	93.22(8)	96.71(11)	96.65(9)		

2.4.1. Cobalt(II) complex (**CoL₂**)

The red solution was slowly evaporated to dryness at room temperature to yield a red solid which was purified by washing with 50 ml of diethyl ether several times and the obtained green precipitate was dried in air. Appropriate single crystals for X-ray crystallography were obtained directly from the reaction mixture. The typical yield was 62%. *Anal.* Calc. for C₂₂H₂₈CoN₂O₂: C, 64.23; H, 6.86; N, 6.81. Found: C, 64.18; H, 7.00; N, 6.89%. Selected IR data (KBr, cm^{−1}): 3056–2900 (w, C–H aliphatic and aromatic), 1601 (ν_{C=N}), 1174 and 1145 (ν_{C–O}).

2.4.2. Copper(II) complex (**CuL₂**)

The resultant red solution was allowed to stand overnight. After concentration at room temperature, a red precipitate was collected by filtration. Appropriate single crystals for X-ray crystallography were obtained directly from the reaction mixture. The typical yield was 87%. *Anal.* Calc. for C₂₂H₂₈CuN₂O₂: C, 63.52; H, 6.78; N, 6.73. Found: C, 63.67; H, 6.81; N, 6.70%. Selected IR data (KBr, cm^{−1}):

3036–2870 (w, C–H aliphatic and aromatic), 1615 (ν_{C=N}), 1181 and 1146 (ν_{C–O}).

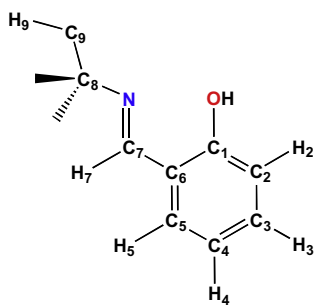
2.4.3. Zinc(II) complex (**ZnL₂**)

The yellow solution was slowly evaporated to dryness at room temperature to yield a yellow solid which was purified by washing with 50 ml of diethyl ether about five times and the obtained yellow precipitate was dried in air. Appropriate single crystals for X-ray crystallography were obtained directly from the reaction mixture. The typical yield was 73%. *Anal.* Calc. for C₂₂H₂₈ZnN₂O₂: C, 63.24; H, 6.75; N, 6.70. Found: C, 63.13; H, 6.67; N, 6.76%. Selected IR data (KBr, cm^{−1}): 3015–2855 (C–H aliphatic and aromatic), 1613 (ν_{C=N}), 1174 and 1148 (ν_{C–O}). ¹H and ¹³C NMR (DMSO-*d*₆, 400 MHz, 298 K): [Table 3](#).

2.4.4. Palladium(II) complex (**PdL₂**)

A green precipitate was collected by filtration and purified by washing with 50 ml of diethyl ether several times and then dried

Table 3
 ^1H and ^{13}C NMR data for the Schiff base ligand (**HL**), **ZnL₂** and **PdL₂** complexes.



	HL	ZnL ₂	PdL ₂		HL	ZnL ₂	PdL ₂
	^1H NMR				^{13}C NMR		
H ₇	8.48(s)	8.52(s)	7.32(s)	C ₁	161.4	169.3	165.0
H ₅	7.44(d of d)	7.40(d)	7.14(d of t)	C ₇	160.9	168.7	159.7
H ₃	7.29(d of t)	7.25(t)	7.17(d of t)	C ₃	131.9	137.1	134.2
H ₂	6.87(d)	6.63(d)	6.80(d)	C ₅	131.8	132.1	133.5
H ₄	6.84(t)	6.56(t)	6.58(d of t)	C ₄	117.9	122.2	119.8
H ₉	1.24(s)	1.25(s)	1.72(s)	C ₆	118.4	118.3	125.6
OH	14.3(s)			C ₂	116.6	113.7	115.4
				C ₈	56.8	59.2	63.2
				C ₉	29.2	29.9	31.6

s, singlet; d, doublet; t, triplet; m, multiplet.

in air. Recrystallization from methanol yielded single crystals of **PdL₂** suitable for X-ray crystallography. The typical yield was 81%. *Anal. Calc.* for $\text{C}_{22}\text{H}_{28}\text{N}_2\text{O}_2\text{Pd}$: C, 57.58; H, 6.15; N, 6.10. *Found*: C, 57.63; H, 6.18; N, 6.19%. Selected IR data (KBr, cm^{-1}): 3011–2864 (w, C–H aliphatic and aromatic), 1607 ($\nu_{\text{C}=\text{N}}$), 1180 and 1148 ($\nu_{\text{C}-\text{O}}$). ^1H and ^{13}C NMR (CDCl_3 , 400 MHz, 298 K): [Table 3](#).

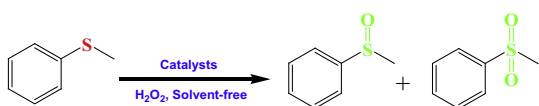
2.5. Catalytic activity and optimization of the reaction conditions

2.5.1. Oxidation of thioanisole with H_2O_2 catalyzed by **CoL₂**, **CuL₂**, **ZnL₂** and **PdL₂** Schiff base complexes

To find the optimized conditions, we investigated the oxidation of thioanisole as a model substrate using hydrogen peroxide ([Scheme 3](#)). The effect of different reaction parameters (H_2O_2 amount, temperature and mmol of catalyst) were studied for the thioanisole oxidation.

2.5.2. General procedure for the catalytic oxidation of sulfides under solvent free conditions

To a mixture of the sulfide (1 mmol) and 30% H_2O_2 (2 mmol), the catalyst (1 mmol) was added and the mixture was stirred at 50 °C for a specified time. The progress of the reaction was monitored by TLC (petroleum ether/ethylacetate 8:3) and GC. After completion of the reaction, the product was extracted with ethyl acetate and the catalyst was separated by filtration. The combined organics were washed with brine (5 ml) and dried over anhydrous



Scheme 3. Oxidation of thioanisole with hydrogen peroxide in the presence of **CoL₂**, **CuL₂**, **ZnL₂** and **PdL₂** Schiff base complexes as catalysts under solvent-free conditions.

Na_2SO_4 . Further purification was achieved by short-column chromatography on silica gel with EtOAc/n-hexane as the eluent.

3. Results and discussion

The Schiff base ligand **HL**, obtained by the self-condensation reaction between *tert*-butylamine and salicylaldehyde in absolute methanol as solvent at ambient temperature and reported in [Scheme 1](#), is a yellow oil, stable in air and moderately soluble in the most common organic solvents. Cobalt(II), copper(II), zinc(II) and palladium(II) Schiff-base complexes were obtained by treating $\text{CoCl}_2 \cdot 6\text{H}_2\text{O}$, $\text{CuCl}_2 \cdot 2\text{H}_2\text{O}$, $\text{Zn}(\text{NO}_3)_2 \cdot 6\text{H}_2\text{O}$ and PdCl_2 with two molar equivalents of the ligand in the presence of triethylamine, respectively ([Scheme 2](#)). The ligand and all the complexes were characterized by elemental analysis (CHN) and FT-IR spectroscopy. Also, the Schiff base ligand and its zinc(II) and palladium(II) complexes were investigated by NMR techniques. The molecular structures of all the complexes were determined by the single crystal X-ray diffraction technique.

3.1. IR spectra

In the FT-IR spectrum of the ligand, a sharp band appeared at 1628 cm^{-1} , which is attributed to the $\text{C}=\text{N}$ vibrations of the imine group [\[42–44\]](#). In the FT-IR spectra of the Schiff base complexes this band was shifted to a lower wavenumber and appeared at 1601, 1615, 1613 and 1607 cm^{-1} for the cobalt(II), copper(II), zinc(II) and palladium(II) complexes, respectively. This shift could be attributed to a weakening of the M–N bonds on adduct formation and this can be explained by the donation of electrons from the nitrogen atom to the empty d-orbitals of the metal atom [\[37,45–47\]](#).

The spectrum of the free ligand shows a strong band at 1196 cm^{-1} , assigned to the phenolic C–O stretching. However, after complexation of the C–O group via the oxygen atom to the metal ion, these bands were observed at 1174 and 1145 cm^{-1} for cobalt(II), 1181 and 1146 cm^{-1} for copper(II), 1174 and 1148 cm^{-1} for zinc(II) and 1180 and 1148 cm^{-1} for the palladium(II) complex. In these complexes, the absence of the phenolic O–H vibration indicates that ligand is deprotonated.

3.2. NMR spectra

The Schiff-base ligand, **HL**, and diamagnetic zinc(II) and palladium(II) complexes, **ZnL₂** and **PdL₂**, were studied by ^1H and ^{13}C NMR experiments ([Table 3](#)). The ^1H and ^{13}C NMR spectra of the ligand and the complexes were run immediately and gave the expected simple spectra, indicating the integrity of the ligand and the complexes. The spectra of the complexes obtained after 12, 24 and 120 h were similar to the initial spectra, indicating that the complexes are stable in solution. The ^1H NMR spectra of the complexes are similar to that of the ligand, but with slight shifts to lower fields. The signal for the imine proton in the zinc(II) and palladium(II) complexes appears at 8.52 and 7.32 ppm, respectively and this downfield shift with respect to the corresponding signal in the free ligand, indicates that the metal–nitrogen bond is retained in solution. Observing no signal corresponding to hydroxyl protons at 14.3 ppm, suggests that the hydroxyl groups are fully deprotonated and the oxygen atoms are most likely coordinated to the metal ions. The ^{13}C NMR spectra show 9 signals for the **ZnL₂** and **PdL₂** complexes. The peak at 168.7 ppm for **ZnL₂** and 159.7 ppm for **PdL₂**, assignable to the imine carbon atoms, confirms the presence of the Schiff base ligand in the complexes [\[48\]](#).

3.3. Description of the crystal structures

3.3.1. Structural description of PdL_2

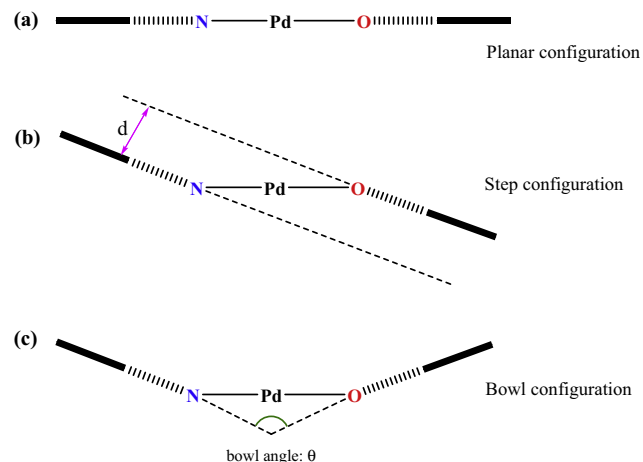
In the solid state, PdL_2 has a crystallographic center of symmetry that is right in the middle point of the palladium(II) ion in a planar-transoid conformation (Fig. 1). The molecular unit is centrosymmetric and is made up of equivalent halves. The *tert*-butyl groups show a fixed conformation in the crystal packing. The molecular structure of PdL_2 is shown in Fig. 1. Selected bond distances and angles are listed in Table 2.

The crystallographic data reveal that the Pd(II) complex has distorted planar configuration and is four-coordinated by two phenolate oxygen and two imine nitrogen atoms of two Schiff base ligands. The ligands coordinated to the Pd(II) center in a *trans* geometry with respect to each other.

The Pd–O distance of 1.987(3) Å and the Pd–N bond length of 2.066(3) Å are similar to those seen in related complexes [49–51]. For instance, distances of 1.979(1) and 1.982(1) Å for the Pd–O bonds and 2.013(1) and 2.015(1) Å for the Pd–N bonds are found in a related di-(2-allyliminomethylphenolato) palladium(II) complex derived from allylamine and salicylaldehyde [51]. The C=N bond distance is 1.285(5) Å (N1=C7), which is consistent with a slight elongation of the C–N double bond when it coordinates to a metal center [50].

The O–Pd–N bond angles [O(1)–Pd(1)–N(1) = 88.45(12)° and O(1)–Pd(1)–N(1A) = 91.55(12)°] are close to 90°. Moreover the coordination of the two NO bidentate chelate ligands to the Pd(II) ion results in the formation of two six-membered rings (Pd(1)/O(1)/C(1)/C(6)/C(7)/N(1) and Pd(1)/O(1A)/C(1A)/C(6A)/C(7A)/N(1A)).

A search for salicylideneimine palladium(II) complexes in the Cambridge Structural Database System 2014 showed that except in one case [52] the *N,O*-ligand atoms in bis(salicylideneimine) palladium(II) complexes, $\text{Pd}(\text{N},\text{O})_2$, adopt a *trans* arrangement in the square planar Pd(II) configuration. For salen-type complexes, $\text{Pd}(\text{ONNO})$, the *N,O*-ligand atoms are *cis* to each other, and they are excluded from the following analysis. The *trans*- $\text{Pd}(\text{N},\text{O})_2$ complexes can subdivide into three classes (Scheme 4): planar configuration (with the distance between the mean planes of the aromatic rings being less than $d = 0.4$ Å, see for example Refs. [53–59]), step configuration (with the distance between the mean



Scheme 4. Planar, step and bowl configurations in bis(salicylideneimine) palladium(II) complexes. —square of Pd, O, and N atoms; — chelate rings; — arene rings.

planes of the aromatic rings greater than $d = 0.4$ Å, see for example Refs. [60–67]) and bowl configuration (see for example Refs. [68–73]).

In the $\text{Pd}(\text{N},\text{O})_2$ complexes with a planar configuration the Pd atom lies in the plane of the chelate rings (see for example Refs. [53–59]). The two six-membered chelate rings and their annulated phenyl rings are coplanar (Scheme 4a). The complexes have an inversion symmetry. Frequently, however, a characteristic feature of $\text{Pd}(\text{N},\text{O})_2$ complexes is an envelope configuration of the six-membered chelate rings, with the Pd atom deviating from the plane of the other 5 atoms of the chelate rings. A direct consequence is the alternative step or a bowl configuration (Scheme 4b and c). In the step configuration the planes between the aromatic rings are parallel to each other (see for example Refs. [60–67]), though complexes still have C_i symmetry. Some Pd(II) complexes adopt a bowl configuration (see for example Refs. [68–73]). At best they have C_2 symmetry. In the PdL_2 complex, the chelate rings have the envelope form and the structure is the step configuration.

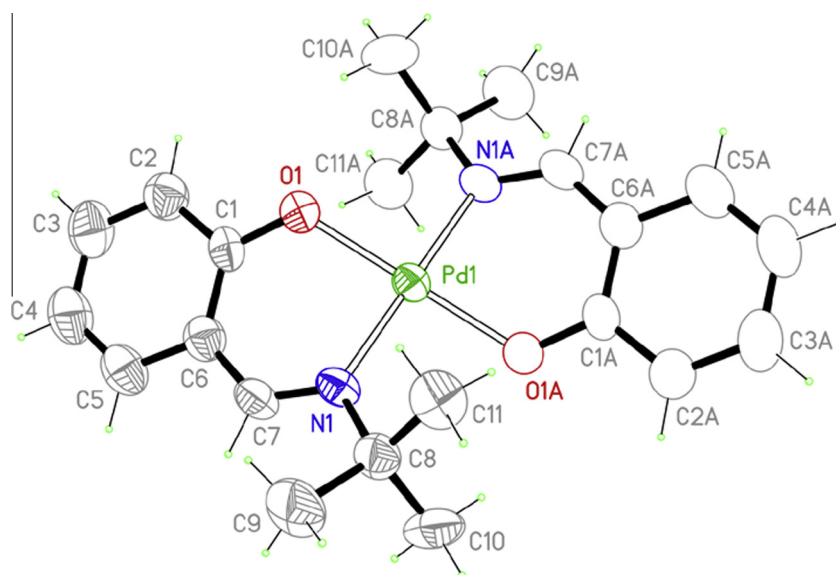


Fig. 1. Perspective view of PdL_2 constituted by the asymmetric unit (filled drawings) showing the numbering scheme and the centrosymmetric half part (empty drawings). Thermal ellipsoids are drawn at the 50% probability level, while the hydrogen size is arbitrary. The suffix A corresponds to the symmetry code $-x, -y, -z$.

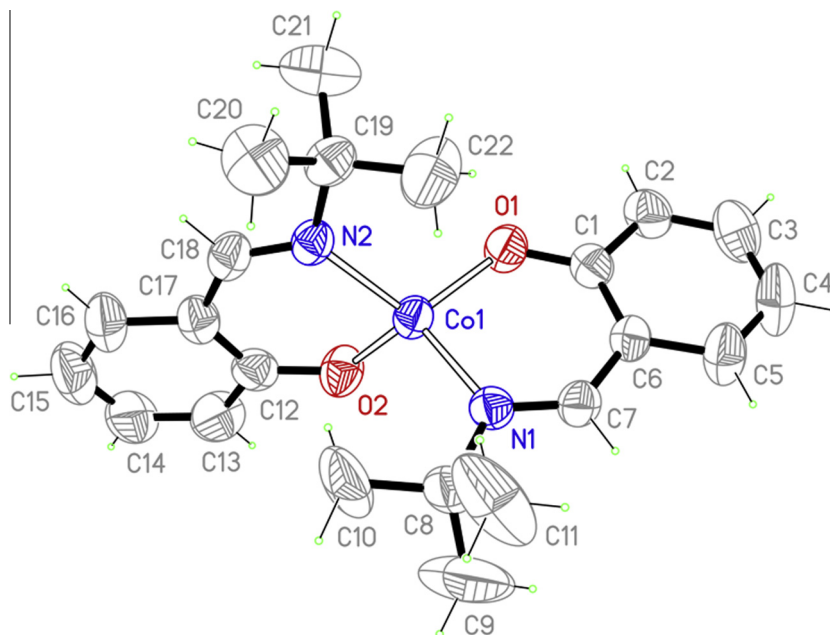


Fig. 2. View of **CoL₂** in the asymmetric unit showing the numbering scheme. Thermal ellipsoids are drawn at the 50% probability level, while the hydrogen size is arbitrary. The C9, C10 and C11 carbon atoms of the *tert*-butyl group are disordered over two sites and refined with site occupancy factors 0.67:0.33. Only the major component of the disordered *tert*-butyl group is shown.

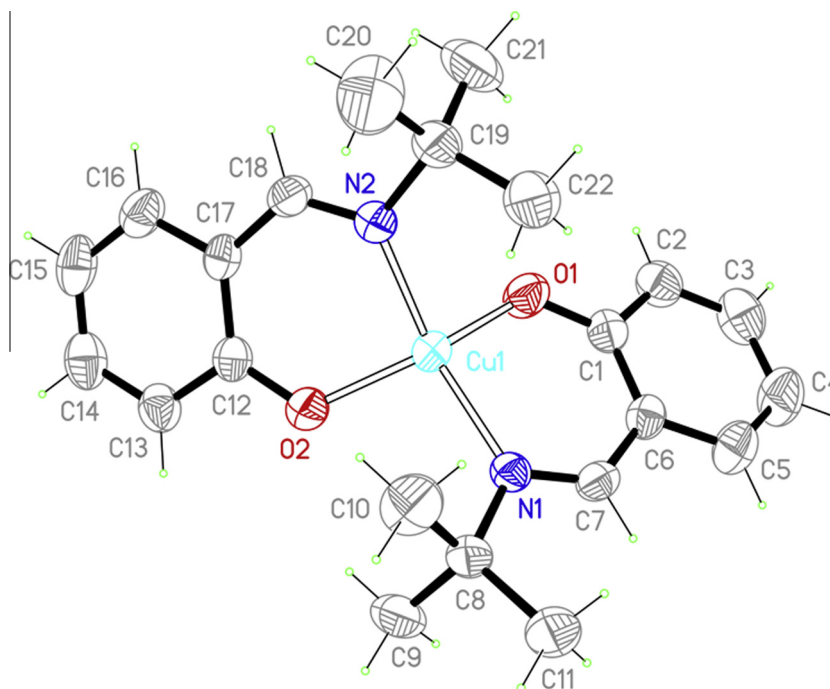


Fig. 3. View of **CuL₂** in the asymmetric unit showing the numbering scheme. Thermal ellipsoids are drawn at the 50% probability level, while the hydrogen size is arbitrary.

3.3.2. Structural description of **CoL₂**, **CuL₂** and **ZnL₂**

An ORTEP view of **CoL₂**, **CuL₂** and **ZnL₂** with the atom-numbering scheme is presented in Figs. 2–4 and the crystallographic data and selected bond lengths and angles are collected in Tables 1 and 2. The crystallographic data reveal that the metal center is four-coordinated by two phenolate oxygen and two imine nitrogen atoms of two Schiff base ligands. The geometry around the metal center is distorted tetrahedral, with *Pca*2(1), *P*2(1)2(1)2(1) and

*P*2(1) space groups for **CoL₂**, **CuL₂** and **ZnL₂**, respectively. The ligands coordinate to the metal center in a *cis* geometry with respect to each other.

The C=N bond distances are 1.272(4) (N1=C7) and 1.281(4) Å (N2=C18) for **CoL₂**, 1.285(3) (N1=C7) and 1.286(3) Å (N2=C18) for **CuL₂** and 1.275(4) (N1=C7) and 1.272(3) Å (N2=C18) for **ZnL₂**, which are consistent with a slight elongation of the C–N double bond when coordinated to a metal center [74].

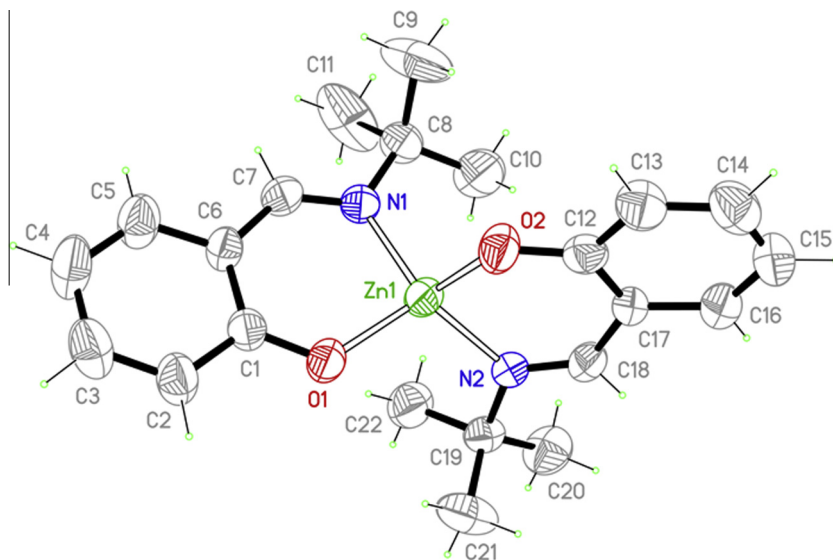


Fig. 4. View of **ZnL₂** in the asymmetric unit showing the numbering scheme. Thermal ellipsoids are drawn at the 50% probability level, while the hydrogen size is arbitrary. The C9, C10 and C11 carbon atoms of the *tert*-butyl group are disordered over two sites and refined with site occupancy factors 0.65:0.35. Only the major component of the disordered *tert*-butyl group is shown.

	$d_{\text{N1-N2}}$	$d_{\text{C8-C19}}$	$\alpha_{\text{N1-M-N2}}$
CoL₂	3.506(5)	4.875(5)	122.03(12)
CuL₂	3.795(4)	5.358(5)	145.58(8)
ZnL₂	3.609(3)	5.025(4)	126.95(13)

Fig. 5. Distances (Å) and angles (°) between the two butyl groups in the **CoL₂**, **CuL₂** and **ZnL₂** complexes.

In the crystal structures of all the complexes, the atoms of the phenyl ring plane [C(1)C(2)C(3)C(4)C(5)C(6) and C(12)C(13)C(14)C(15)C(16)C(17)] and the chelate ring formed by the same ligand plane [O(1)/M(1)/N(1)/C(7)/C(6)/C(1) and O(2)/M(1)/N(2)/C(18)/C(17)/C(12)] are nearly coplanar with dihedral angles of 3.82(16)° and 2.17(19)° for **CoL₂**, 2.53 (12)° and 11.13 (11)° for **CuL₂** and 5.48 (13)° and 5.00 (11)° for **ZnL₂**, respectively.

Examination of the main metal–ligand distances shows that the Co···N, Cu···N and Zn···N distances are longer than the Co···O, Cu···O and Zn···O distances. The M···N and M···O distances are 2.003(3) and 1.883(3) Å for **CoL₂**, 1.995(2) and 1.8957(17) Å for **CuL₂** and 2.0200(19) and 1.911(2) Å for **ZnL₂**.

As depicted in Figs. 2–4, all of the complexes have a distorted tetrahedral geometry, with bidentate coordinated ligands which have a *cis* geometry with respect to each other. The N(1)–M–N(2) angle in **CuL₂** is larger than that for the **CoL₂** and **ZnL₂** complexes (Fig. 5). With such an angle in **CuL₂**, the distance and steric hindrance between the two butyl groups in **CuL₂** are greater and lower respectively than in the **CoL₂** and **ZnL₂** complexes.

The N–M–O bond angles (bite angle) are 97.94(12) [O(1)–Co(1)–N(1)] and 96.71(11)° [O(2)–Co(1)–N(2)] in the **CoL₂** complex, 95.88(8) [O(1)–Cu(1)–N(1)] and 93.22(8)° [O(2)–Cu(1)–N(2)] in the **CuL₂** complex and 97.58(11) [O(1)–Zn(1)–N(1)] and 96.65(9)° [O(2)–Zn(1)–N(2)] in the **ZnL₂** complex.

Three-dimensional structures of Cu(II) complexes with naphthalaldimines and salicylaldimines found in the Cambridge Structural Database (CSD) were investigated by Costamagna and

co-workers and showed a large variation in the dihedral angle between the planes N(1)–Cu(1)–O(1) and N(2)–Cu(1)–O(2) [75]. The results show that bulky R groups induce large *Dih* values. It can be seen that packing effects influence the structural features. Thus, bis[N-(cyclooctyl)-2-oxy-1-naphthaldi-minato]copper(II) has a bulky *c*-octyl substituent (*c* stands for cyclo) that determines a flat-tetrahedral coordination sphere [76]. Thus, steric hindrance of the N substituents is not the only factor influencing the coordination sphere in the solid state.

In our case, **CuL₂** is more distorted than bis(N-*tert*-butyl-2-oxy-1-naphthalaldimino)copper(II), according to their *Dih* values of 53.6° and 45.4°, respectively [75]. In **CoL₂** and **ZnL₂**, the dihedral angle between the planes N(1)–M(1)–O(1) and N(2)–M(1)–O(2) are 87.1° and 83.1°, respectively, and the two bidentate ligands in these complexes are almost perpendicular to each other.

3.4. Electronic spectra

Electronic spectra of the free schiff base ligand and the complexes were recorded in a CHCl₃ solution. The absorption spectra for the Schiff base ligand (**H₂L**) and all the complexes are shown in Fig. 6. The electronic spectrum of the Schiff base ligand exhibits three main peaks at 255, 316 and 409 nm with a shoulder at 240 nm (Fig. 6). The first and second peaks (240 and 255 nm) are attributed to benzene $\pi \rightarrow \pi^*$ transitions. The azomethine $\pi \rightarrow \pi^*$ and $n \rightarrow \pi^*$ transitions are viewed at 316 and at 409 nm as broad peaks with low intensity, respectively [77].

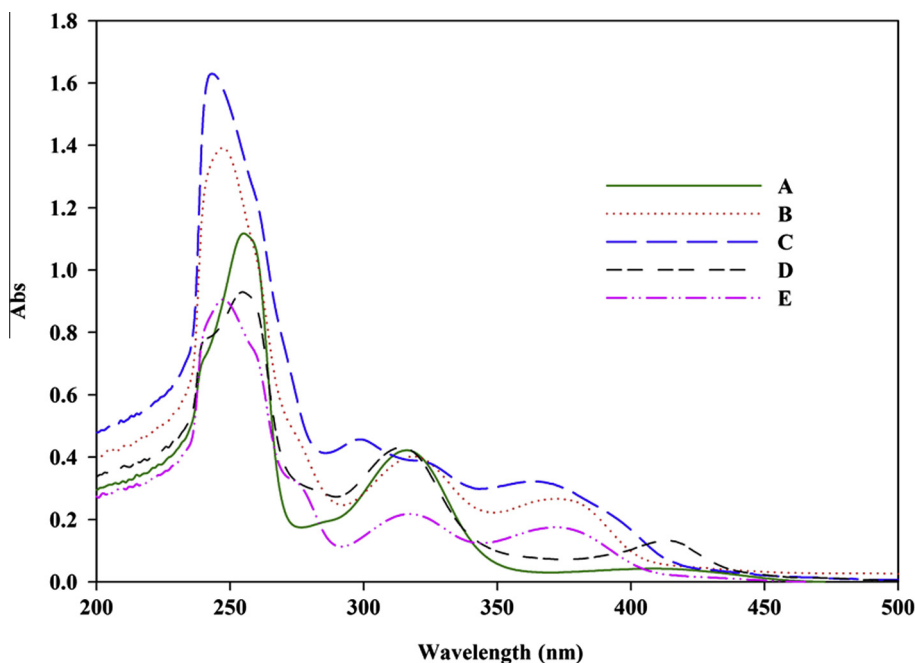


Fig. 6. Electronic spectra of the schiff base ligand and the complexes (A: H_2L , B: CuL_2 , C: CoL_2 , D: PdL_2 , E: ZnL_2).

Table 4

Oxidation of thioanisole with different amounts of catalyst in the presence H_2O_2 .^a

Entry	Catalyst	mmol of catalyst	Conversion (%) ^b	Selectivity (%) ^c
1	Co	0.001	20	97
2	Co	0.005	23	99
3	Co	0.01	29	99
4	Co	0.05	30	99
5	Cu	0.001	48	94
6	Cu	0.005	61	99
7	Cu	0.01	80	99
8	Cu	0.05	83	99
9	Zn	0.001	63	98
10	Zn	0.005	79	99
11	Zn	0.01	93	99
12	Zn	0.05	93	99
13	Pd	0.001	52	96
14	Pd	0.005	60	99
15	Pd	0.01	74	99
16	Pd	0.05	76	99
17	None	–	16	75

^a Reaction conditions: thioanisole (1 mmol) and H_2O_2 (2 mmol) at 50 °C for 3 h.

^b Conversion based on sulfide substrates.

^c Selectivity for sulfone.

In the complexes CoL_2 , CuL_2 , ZnL_2 and PdL_2 , the broad band that appears in the range 350–450 nm with more intensity than free Schiff base ligand may be due to MLCT (comprised of a transition between the metal centered HOMO to the ligand centered LUMO ($\text{C}=\text{N}(\pi^*)$), LMCT, d-d and azomethine $n \rightarrow \pi^*$ transitions. This band is in the range usually observed for azomethine $n \rightarrow \pi^*$, d-d and LMCT transitions [36,78]. According to the d^{10} electronic configuration (+2 formal oxidation state) of zinc, the Zn(II) complex shows no d-d transition.

3.5. Catalytic activity of the different complexes in the solvent free oxidation of sulfides

3.5.1. Influence of different amounts of catalyst

We first studied the oxidation of thioanisole as a model substrate using 30% aqueous hydrogen peroxide as the oxidant under

Table 5

Oxidation of thioanisole with various amounts of H_2O_2 in the presence of Co, Ni, Zn and Pd schiff base^a complexes.

Entry	Catalyst	mmol H_2O_2	Conversion (%) ^b	Selectivity (%) ^c
1	Co	0.5	17	66
2	Co	1	20	81
3	Co	2	29	99
4	Co	4	35	99
5	Cu	0.5	33	58
6	Cu	1	51	77
7	Cu	2	80	99
8	Cu	4	86	99
9	Zn	0.5	37	63
10	Zn	1	59	72
11	Zn	2	93	99
12	Zn	4	96	99
13	Pd	0.5	30	69
14	Pd	1	50	80
15	Pd	2	74	99
16	Pd	4	77	99

^a Reaction conditions: Thioanisole (1 mmol), Catalyst (0.01 mmol) and H_2O_2 30% at 50 °C for 3 h.

^b Conversion based on sulfide substrates.

^c Selectivity for sulfone.

solvent-free conditions. The amount of catalyst had a considerable effect on the conversion of thioanisole to the corresponding sulfone. The results are given in Table 4 and show that the reaction is sensitive to the catalyst amounts for each case. These results showed that on increasing the catalyst amount, the reaction conversion enhances without significant changing the selectivity for all the catalysts. The role of the catalyst is very important in the reaction because this reaction has low conversion without any catalyst (Table 4, entry 17). Also, among the four catalysts, ZnL_2 showed a better catalytic performance compared to the others.

3.5.2. Influence of different amounts of oxidant

After optimization of the catalyst amount, we demonstrated the effect of the amount of oxidant on the oxidation of thioanisole in

Table 6Oxidation of thioanisole with different catalysts at various temperatures.^a

Entry	Catalyst	Temperature (°C)	Conversion (%) ^b	Selectivity (%) ^c
1	Co	25	16	45
2	Co	50	29	99
3	Co	60	31	99
4	Co	85	43	99
5	Cu	25	41	43
6	Cu	50	80	99
7	Cu	60	82	99
8	Cu	85	91	99
9	Zn	25	46	47
10	Zn	50	93	99
11	Zn	60	96	99
12	Zn	85	99	99
13	Pd	25	37	56
14	Pd	50	74	99
15	Pd	60	77	99
16	Pd	85	84	99

^a Reaction conditions: thioanisole (1 mmol), H₂O₂ (3 mmol), 0.01 mmol catalyst for 3 h.^b Conversion based on sulfide substrates.^c Selectivity for sulfone.

the presence of each of the four catalysts. With 0.5 mmol of H₂O₂ all catalysts showed low conversions (entries 1, 5, 9 and 13, Table 5); in contrast, on raising the amount of oxidant, higher conversions were obtained; among them all, **ZnL₂** provided the highest conversion of 99% and selectivity of 99%. Furthermore, it can be seen in Table 5 that with an increase in the amount of the H₂O₂ with 0.01 mmol catalyst at 50 °C, the conversion of thioanisole increased, but selectivity for sulfoxide decreased quickly.

3.5.3. Influence of reaction temperature

In the present work for optimization of the reaction conditions, we also studied the effect of temperature on the catalytic performance of **CoL₂**, **CuL₂**, **ZnL₂** and **PdL₂** (Table 6). Obviously, a substantially improved conversion of thioanisole to the corresponding sulfone and sulfoxide was observed with an increase in the temperature, but in all cases a decrease in

selectivity to sulfoxide was observed; for example at 85 °C, an increase in the oxidation activity was observed, which caused the increased formation of the methyl phenyl sulfone, but selectivity for sulfoxide decreased for all catalysts.

3.5.4. Influence of the geometrical structure of the catalyst

In this work, the catalytic activity of four kinds of metal complexes were examined (Figs. 7–10). Among them, **ZnL₂** showed the best catalytic activity for the oxidation of sulfide and **CoL₂** showed the lowest catalytic performance under these reaction conditions. In general, there are some different parameters affecting the performance of a catalyst. Here, we studied the influence of the geometrical structure of the metal complex. As previously reported [79–81], formation of a metal-peroxo intermediate occurs in some oxidation reactions that shows the geometrical structure of the complex plays an important role in its catalytic activity. In the present study, according to Fig. 5, the **CoL₂** complex has more steric hindrance around the metal center due to the geometry of the ligands. So the bulkiness of the ligands for **CoL₂** probably lead to a further lowering of the accessibility of the metal center in the catalyst and so reduce the catalytic efficiency of the complex (the slope of the conversion curve for this complex is lower than for the other ones) (Figs. 7–10).

3.6. Oxidation of different sulfides

The oxidation of thioanisole to the corresponding sulfone, catalyzed by **CoL₂**, **CuL₂**, **ZnL₂** and **PdL₂** with 2 mmol of H₂O₂ at 50 °C, was determined as a function of the reaction time (Figs. 7–10). The results indicate that at the beginning of the reaction the sulfoxide is formed selectively, but the amount of sulfone increases slightly over time. It is remarkable that sulfone can be obtained with high selectivity with 2 equivalents of 30% H₂O₂ in the presence of all the complexes in 3 h under solvent free conditions.

In an effort to extend the scope of the reaction under the optimized conditions, the **CuL₂**, **ZnL₂** and **PdL₂** catalysts were applied to the oxidation of various types of aliphatic and aromatic sulfides

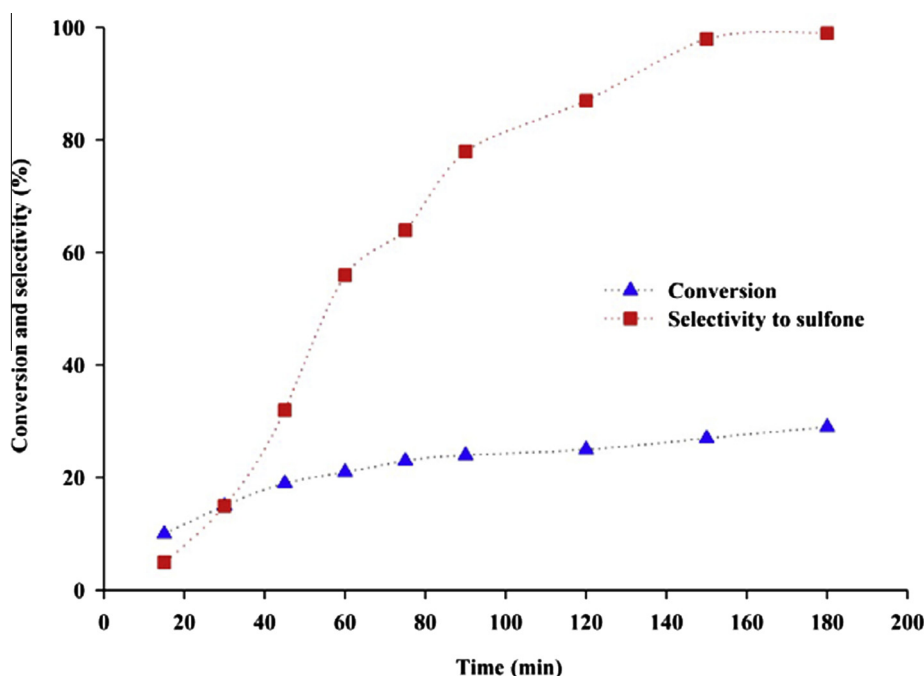


Fig. 7. Reaction profile of the oxidation of thioanisole catalyzed by **CoL₂** with 2 mmol of H₂O₂ at 50 °C.

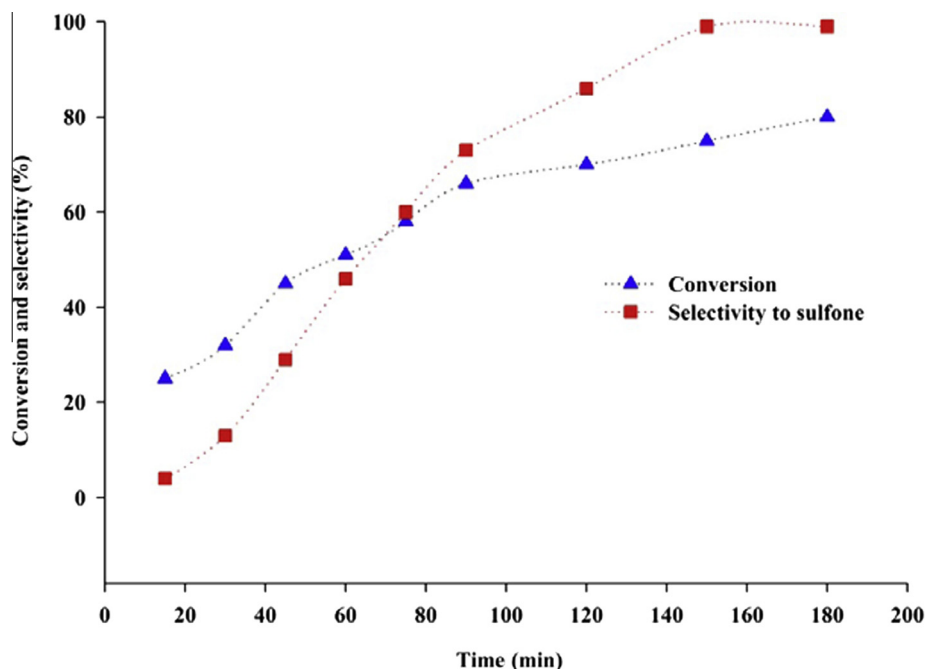


Fig. 8. Reaction profile of the oxidation of thioanisole catalyzed by CuL_2 with 2 mmol of H_2O_2 at 50 °C.

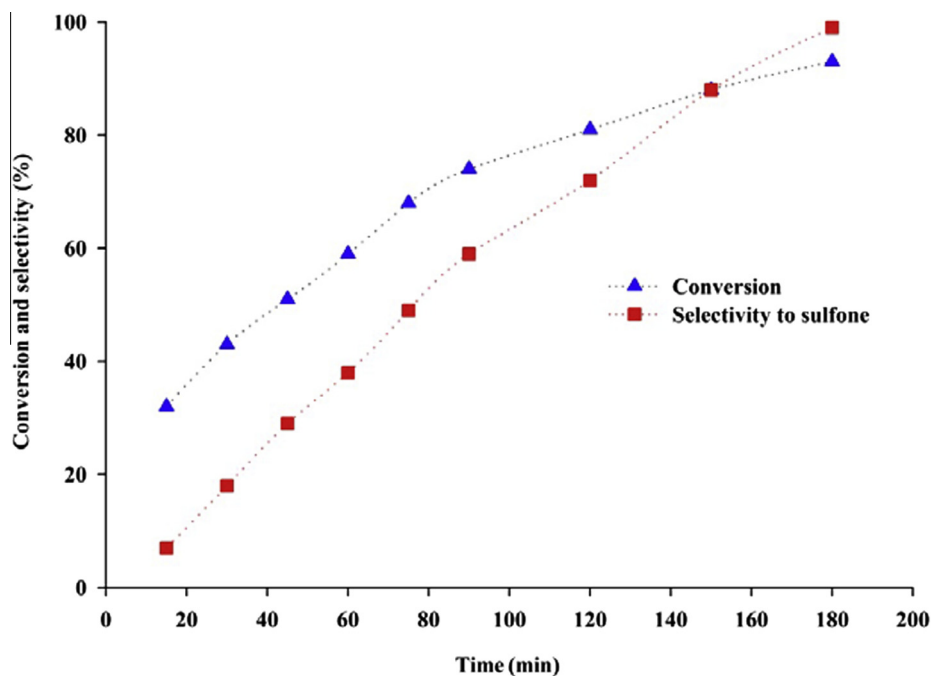


Fig. 9. Reaction profile of the oxidation of thioanisole catalyzed by ZnL_2 with 2 mmol of H_2O_2 at 50 °C.

and the results are summarized in Table 7. CoL_2 did not show good catalytic activity, for this reason we did not use it for oxidation of different sulfides. The different sulfides were selectively oxidized to the corresponding sulfones with 2 mmol H_2O_2 under solvent free conditions. The oxidation of allylsulfides and hydroxysulfides proceeded chemoselectively to the corresponding sulfones, without the epoxidation of the double bonds and dehydrogenation of the hydroxyl groups (entries 6, 7 and 8). Thioanisole was oxidized

under solvent-free conditions to the corresponding sulfone in 93% yield with 2 mmol H_2O_2 and ZnL_2 as a catalyst (Table 7, entry 2). The CuL_2 catalyst gave sulfone in 80% conversion, while the PdL_2 catalyst gave methyl phenyl sulfone in 74% conversion (Table 7, entry 2). Dibutyl sulfide, thiophene and all the aromatic sulfides, such as methylphenyl sulfide, diphenyl sulfide and the substituted diphenyl sulfide (4-nitro), were oxidized to the corresponding sulfones with a good conversion in the presence of each of the three

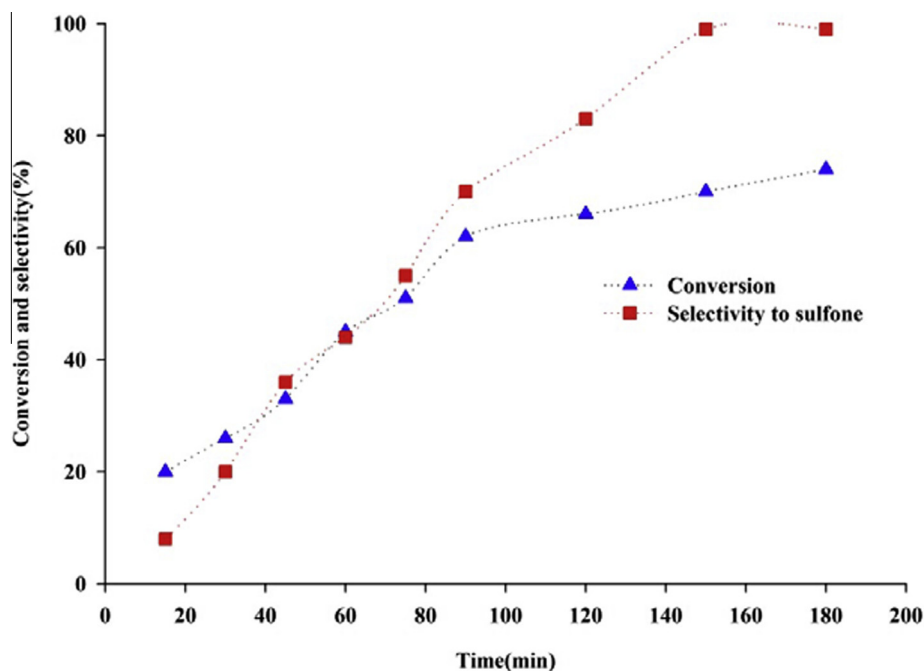
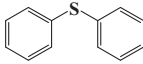
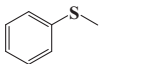
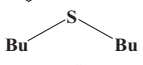
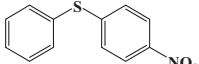

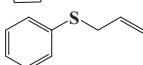
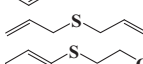
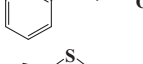
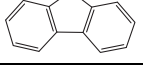


Fig. 10. Reaction profile of the oxidation of thioanisole catalyzed by PdL_2 with 2 mmol of H_2O_2 at 50°C .

Table 7

The oxidation of various sulfides with CoL_2 , CuL_2 , ZnL_2 , and PdL_2 Schiff-base complexes as catalyst using 30% aqueous H_2O_2 .^a

Entry	Sulfide	Time (h)	Conversion (%) ^b			Selectivity(%) ^c
			CuL_2	ZnL_2	PdL_2	
1		4.5	83	96	79	99
2		3	80	93	74	99
3		5.5	85	97	78	99
4		5.3	71	92	77	98
5		3.15	76	97	81	99
6		5	79	95	76	99
7		7	80	98	79	98
8		5	76	92	69	99
9		5.5	22	29	25	99

^a Reaction conditions: catalyst (0.01 mmol), substrate (1.0 mmol), H_2O_2 (2 mmol), solvent free, at 50°C .

^b Conversion based on sulfide substrates.

^c Selectivity for sulfone.

catalysts (Table 7, entries 1–5). Unfortunately, with this protocol DBT was oxidized into sulfone (Table 7, entry 9) with a low conversion. Although DBT was oxidized into sulfone with low conversion under the reaction conditions, these results show the good capability of this method for the oxidation of several types of sulfides to the corresponding sulfones.

4. Conclusion

In conclusion, we have synthesized a new bidentate NO donor ligand and its Co(II), Cu(II), Zn(II) and Pd(II) complexes. The structures of the complexes have been established using single crystal X-ray diffraction analysis. The Co(II), Cu(II), Zn(II) and Pd(II) atoms

are coordinated by two phenolic-O atoms and two azomethine-N atoms to form a distorted tetrahedral geometry for the **CoL₂**, **CuL₂** and **ZnL₂** complexes and square-planar geometry for **PdL₂**.

We have demonstrated the effectiveness of these complexes as catalysts for the green oxidation of sulfides to the corresponding sulfones with hydrogen peroxide. In this system the reactions can be carried out under solvent-free conditions as a green sustainable method using all the catalysts in the presence of H₂O₂. Conversions of 20–96%, and selectivities of 98–100% for sulfone are observed with the four compounds as catalysts. Also, we found that **ZnL₂** shows a better catalytic activity for the oxidation of sulfide and **CoL₂** shows a lower catalytic performance with these reaction conditions. Overall, we recommend this green, simple, clean, and economical procedure for the oxidation of different sulfides to the corresponding sulfones.

Acknowledgement

Support for this research by the University of Isfahan is acknowledged.

Appendix A. Supplementary data

CCDC 1045369, 1045370, 1045371 and 1045372 contain the supplementary crystallographic data for **CoL₂**, **CuL₂**, **PdL₂** and **ZnL₂**, respectively. These data can be obtained free of charge via <http://www.ccdc.cam.ac.uk/conts/retrieving.html>, or from the Cambridge Crystallographic Data Centre, 12 Union Road, Cambridge CB2 1EZ, UK. Fax: +44 1223 336 033; or e-mail: deposit@ccdc.cam.ac.uk.

References

- [1] M.C. Carreno, *Chem. Rev.* 95 (1995) 1717.
- [2] E.N. Prilezhaeva, *Russ. Chem. Rev.* 70 (2001) 897.
- [3] I. Fernandez, N. Khair, *Chem. Rev.* 103 (2003) 3651.
- [4] A.J. Mancuso, D. Swern, *Synthesis* (1981) 165.
- [5] V.Y. Kukushkin, *Coord. Chem. Rev.* 139 (1995) 375.
- [6] K. Kamata, T. Hirano, M. Mizuno, *Chem. Commun.* (2009) 3958.
- [7] (a) B. Karimi, M. Ghoreishi-Nezhad, J.H. Clark, *Org. Lett.* 7 (2005) 625; (b) R. Noyori, M. Aoki, K. Sato, *Chem. Commun.* (2003) 1977.
- [8] K. Jeyakumar, R.D. Chakravarthy, D.K. Chand, *Catal. Commun.* 10 (2009) 1948.
- [9] R.A. Sheldon, J.K. Kochi, *Metal Catalyzed Oxidations of Organic Compounds*, Academic Press, London, 1981.
- [10] R. Afrasiabi, M.R. Farsani, B. Yadollahi, *Tetrahedron Lett.* 55 (2014) 3923.
- [11] (a) R. Noyori, *Chem. Commun.* (2005) 1807; (b) K. Jeyakumar, D.K. Chand, *Tetrahedron Lett.* 47 (2006) 4573; (c) K. Kaczorowska, Z. Kolarska, K. Mitka, P. Kowalski, *Tetrahedron* 61 (2005) 8315.
- [12] (a) N. Gharah, S. Chakraborty, A.K. Mukherjee, R. Bhattacharyya, *Inorg. Chim. Acta* 362 (2009) 1089; (b) S.K. Maiti, S. Banerjee, A.K. Mukherjee, K.M.A. Malik, R. Bhattacharyya, *New J. Chem.* 29 (2005) 554; (c) S. Choi, J.D. Yang, M. Ji, H. Choi, M. Kee, K.H. Ahn, S.H. Byeon, W. Baik, S. Koo, *J. Org. Chem.* 66 (2001) 8192.
- [13] M. Ciclosi, C. Dinioi, L. Gonsalvi, M. Peruzzini, E. Manoury, R. Poli, *Organometallics* 27 (2008) 2281.
- [14] C.A. Gamelas, T. Lourenc, O.A.P. da Costa, A.L. Simpício, C.C. Romao, *Tetrahedron Lett.* 49 (2008) 4708.
- [15] P. Gogoi, M. Kalita, T. Bhattacharjee, P. Barman, *Tetrahedron Lett.* 55 (2014) 1028.
- [16] Y. Wang, M. Wang, Y. Wang, X. Wang, L. Wang, L. Sun, *J. Catal.* 273 (2010) 177.
- [17] G. Romanowski, J. Kira, *Polyhedron* 53 (2013) 172.
- [18] K.M. Kadish, K.M. Smith, R. Guilard (Eds.), *The Porphyrin Handbook*, Biochemistry and Binding: Activation of Small Molecules, vol. 4, Academic Press, 2000.
- [19] V. Hulea, A.L. Maciucă, F. Fajula, E. Dumitriu, *Appl. Catal. A* 313 (2006) 200.
- [20] (a) J.H. Clark, *Green Chem.* 1 (1999) 1; (b) I. Arends, R. Sheldon, U. Hanefeld, *Green Chemistry and Catalysis*, Wiley-VCH Verlag GmbH & Co. KGaA, Weinheim, 2007.
- [21] R.H. Holm, *J. Am. Chem. Soc.* 82 (1960) 5632.
- [22] A.D. Garnovskii, A.P. Sadimenko, M.I. Sadimenko, D.A. Garnovskii, *Coord. Chem. Rev.* 173 (1998) 31.
- [23] S.D. Bella, G. Consiglio, S. Sortino, G. Giancane, L. Valli, *Eur. J. Inorg. Chem.* 33 (2008) 5228.
- [24] Ch.T. Lyons, T.D.P. Stack, *Coord. Chem. Rev.* 257 (2013) 528.
- [25] P.G. Cozzi, *Chem. Soc. Rev.* 33 (2004) 410.
- [26] S. Yamada, *Coord. Chem. Rev.* 190–192 (1999) 537.
- [27] K.C. Gupta, A.K. Sutar, *Coord. Chem. Rev.* 252 (2013) 1420.
- [28] S. Sarkar, S. Biswas, M.S. Liao, T. Kar, Y. Aydogdu, F. Dagdelen, G. Mostafa, A.P. Chattopadhyay, G.P.A. Yap, R.-H. Xie, A.T. Khan, K. Dey, *Polyhedron* 27 (2008) 3359.
- [29] G. Barone, A. Terenzi, A. Lauria, A.M. Almerico, J.M. Leal, N. Busto, B. García, *Coord. Chem. Rev.* 257 (2013) 2848.
- [30] M. De Rosa, M. Lamberti, C. Pellicchia, A. Scettri, R. Villano, A. Soriente, *Tetrahedron Lett.* 47 (2006) 7233.
- [31] M. Palucki, P. Hanson, E.N. Jacobsen, *Tetrahedron Lett.* 33 (1992) 7111.
- [32] C. Bolm, F. Bienewald, *Synlett* (1998) 1327.
- [33] Y.C. Jeong, S. Choi, Y.D. Hwang, K.H. Ahn, *Tetrahedron Lett.* 45 (2004) 9249.
- [34] H. Iranmanesh, M. Behzad, G. Bruno, H. Amiri Rudbari, H. Nazari, A. Mohammadi, O. Taheri, *Inorg. Chim. Acta* 395 (2013) 81.
- [35] M. Pooyan, A. Ghaffari, M. Behzad, H. Amiri Rudbari, G. Bruno, *J. Coord. Chem.* 66 (2013) 4255.
- [36] A. Ghaffari, M. Behzad, M. Pooyan, H. Amiri Rudbari, G. Bruno, *J. Mol. Struct.* 1063 (2014) 1.
- [37] G. Grivani, G. Bruno, H. Amiri, A.D. Khalaji, P. Pourteimouri, *Inorg. Chem. Commun.* 18 (2012) 15.
- [38] X-AREA, Version 1.30, Program for the Acquisition and Analysis of Data, Stoe & Cie GmbH, Darmstadt, Germany, 2005.
- [39] (a) X-RED, Version 1.28b, Program for Data Reduction and Absorption Correction, Stoe & Cie GmbH, Darmstadt, Germany, 2005; (b) X-SHAPE, Version 2.05, Program for Crystal Optimization for Numerical Absorption Correction, Stoe & Cie GmbH, Darmstadt, Germany, 2004.
- [40] M.C. Burla, R. Caliendo, M. Camalli, B. Carrozzini, G.L. Casciaro, L. De Caro, C. Giacovazzo, G. Polidori, R. Spagna, *J. Appl. Crystallogr.* 38 (2005) 381.
- [41] G.M. Sheldrick, *Acta Cryst. A* 64 (2008) 112.
- [42] H. Amiri Rudbari, A. Varasteh Moradi, *Synthesis* (2010) 205.
- [43] H. Keypour, H. Amiri Rudbari, R. Azadbakht, *Synth. Commun.* 40 (2010) 1486.
- [44] H. Amiri Rudbari, A. Varasteh Moradi, R. Azadbakht, *Synth. Commun.* 41 (2011) 528.
- [45] G. Grivani, V. Tahmasebi, K. Eskandari, A. Dehno Khalaji, G. Bruno, H. Amiri Rudbari, *J. Mol. Struct.* 1054 (2013) 100.
- [46] H. Keypour, M. Shayeesteh, D. Nematollahi, L. Valencia, H. Amiri Rudbari, *J. Coord. Chem.* 63 (2010) 4165.
- [47] G. Grivani, M. Vakili, A.D. Khalaji, G. Bruno, H. Amiri Rudbari, M. Taghavi, V. Tahmasebi, *J. Mol. Struct.* 1072 (2014) 77.
- [48] H. Keypour, H. Amiri Rudbari, R. Azadbakht, E. Abouzari Lotf, *J. Chem. Res.* (2009) 361.
- [49] R.R. Coombs, M.K. Ringer, J.M. Blacquire, J.C. Smith, J.S. Neilsen, Y.-S. Uh, J.B. Gilbert, L.J. Leger, H. Zhang, A.M. Irving, S.L. Wheaton, C.M. Vogels, S.A. Westcott, A. Decken, F.J. Baerlocher, *Transition Met. Chem.* 30 (2005) 411.
- [50] I. Aiello, A. Crispini, M. Ghedini, M. La Deda, F. Barigelli, *Inorg. Chim. Acta* 308 (2000) 121.
- [51] S.C. Bhatia, J.M. Bindlish, A.R. Saini, P.C. Jain, *J. Chem. Soc., Dalton Trans.* (1981) 1773.
- [52] B.J. Tardiff, J.C. Smith, S.J. Duffy, C.M. Vogels, A. Decken, S.A. Westcott, *Can. J. Chem.* 85 (2007) 392.
- [53] H. Bahron, A.M. Tajuddin, W.N.W. Ibrahim, M. Hemamalini, H.-K. Fun, *Acta Crystallogr., Sect. E* 67 (2011) m759.
- [54] O.A. Blackburn, B.J. Coe, J. Fielden, M. Helliwell, J.J.W. McDouall, M.G. Hutchings, *Inorg. Chem.* 49 (2010) 9136.
- [55] J.-Y. Li, C.-X. Liu, P. Li, Huaxue Yanjiu 17 (2006) 36.
- [56] M.D. Hall, T.W. Failes, D.E. Hibbs, T.W. Hambley, *Inorg. Chem.* 41 (2002) 1223.
- [57] H. Brunner, M. Niemetz, M. Zabel, *Z. Naturforsch. B55* (2000) 145.
- [58] T. Tsuno, H. Iwabe, H. Brunner, *Inorg. Chim. Acta* 400 (2013) 262.
- [59] K.J. Miller, J.H. Baag, M.M. Abu-Omar, *Inorg. Chem.* 38 (1999) 4510.
- [60] M. Bagherzadeh, M. Amini, A. Ellern, L.K. Woo, *Inorg. Chim. Acta* 383 (2012) 46.
- [61] E.C. Bowes, G.M. Lee, C.M. Vogels, A. Decken, S.A. Westcott, *Inorg. Chim. Acta* 377 (2011) 84.
- [62] R. Zhong, Y.-N. Wang, X.-Q. Guo, Z.-X. Chen, X.-F. Hou, *Chem. Eur. J.* 17 (2011) 11041.
- [63] U. Caruso, B. Panunzi, A. Roviello, M. Tingoli, A. Tuzi, *Inorg. Chem. Commun.* 14 (2011) 46.
- [64] Z. Gan, K. Kawamura, K. Eda, M. Hayashi, *J. Organomet. Chem.* 695 (2010) 2022.
- [65] A.M. Tajuddin, H. Bahron, W.N.W. Ibrahim, B.M. Yamin, *Acta Crystallogr., Sect. B* 66E (2010) m1100.
- [66] S.-Y. Li, C.-J. Chen, P.-Y. Lo, H.-S. Sheu, G.-H. Lee, C.K. Lai, *Tetrahedron* 66 (2010) 6101.
- [67] Y.-C. Lai, H.-Y. Chen, W.-C. Hung, C.-C. Lin, F.-E. Hong, *Tetrahedron* 61 (2005) 9484.
- [68] U. Caruso, R. Diana, B. Panunzi, A. Roviello, M. Tingoli, A. Tuzi, *Inorg. Chem. Commun.* 12 (2009) 1135.
- [69] T. Naota, H. Koori, *J. Am. Chem. Soc.* 127 (2005) 9324.
- [70] A.W. Maverick, R.K. Laxman, M.A. Hawkins, D.P. Martone, F.R. Fronczek, *Dalton Trans.* (2005) 200.
- [71] H. Li, Y.-J. Wu, C. Xu, R.-Q. Tian, *Polyhedron* 26 (2007) 4389.
- [72] H. Houjou, N. Schneider, Y. Nagawa, M. Kanesato, R. Hirotsu, *Eur. J. Inorg. Chem.* (2004) 4216.

- [73] M. Gomez-Simon, S. Jansat, G. Muller, D. Panyella, M. Font-Bardia, X. Solans, J. Chem. Soc., Dalton Trans. (1997) 3755.
- [74] M. Khorshidifard, H. Amiri Rudbari, Z. Kazemi-Delikani, V. Mirkhani, R. Azadbakht, J. Mol. Struct. 1081 (2015) 494.
- [75] M. Villagrán, F. Caruso, M. Rossi, J.H. Zagal, J. Costamagna, Eur. J. Inorg. Chem. (2010) 1373.
- [76] M. Aguilar-Martinez, R. Saloma-Aguilar, N. Macias-Ruvalcaba, R. Cetina-Rosado, A. Navarrete-Vazquez, V. Gomez-Vidales, A. Zentella-Dehesa, R.A. Toscano, S. Hernandez-Ortega, J.M. Fernandez-G, J. Chem. Soc., Dalton Trans. (2001) 2346.
- [77] B. Shafaatian, Z. Ozbakzaei, B. Notash, S.A. Rezvani, Spectrochim Acta, Part A 140 (2015) 248.
- [78] N. Sumita Rao, M.N. Jaiswal, D.D. Mishra, R.C. Maurya, Polyhedron 12 (1993) 2045.
- [79] R. Ando, T. Yagyu, M. Maeda, Inorg. Chim. Acta 357 (2004) 2237.
- [80] A. Rezaeifard, M. Jafarpour, A. Naeimi, M. Salimi, Inorg. Chem. Commun. 15 (2012) 230.
- [81] G. Romanowski, J. Kira, M. Wera, Polyhedron 67 (2014) 529.